Low-temperature phase transformation of CZTS thin films*

Wei Zhao(赵蔚)[1,2], Lin-Yuan Du(杜霖元)[1], Lin-Lin Liu(刘林林)[1], Ya-Li Sun(孙亚利)[1], Zhi-Wei Liu(柳志伟)[1], Xiao-Yun Teng(滕晓云)[1], Juan Xie(谢娟)[2], Kuang Liu(刘匡)[3], Wei Yu(于威)[1,†], Guang-Sheng Fu(傅广生)[1,‡], and Chao Gao(高超)[4,§]

[1] *Hebei Key Laboratory of Optic-electronic Information Materials, College of Physics Science and Technology, Hebei University, Baoding* 071002, *China*
[2] *School of Science, Hebei University of Engineering, Handan* 056038, *China*
[3] *School of Microelectronics and Solid State Electronics, University of Electronic Science and Technology of China, Chengdu* 610054, *China*
[4] *Institute of Photovoltaics, Nanchang University, Nanchang* 330031, *China*

(Received 4 December 2016; revised manuscript received 13 February 2017; published online 10 March 2017)

The low temperature phase transformation in the Cu_2ZnSnS_4 (CZTS) films was investigated by laser annealing and low temperature thermal annealing. The Raman measurements show that a-high-power laser annealing could cause a red shift of the Raman scattering peaks of the kesterite (KS) structure and promotes the formation of the partially disordered kesterite (PD-KS) structure in the CZTS films, and the low-temperature thermal annealing only shifts the Raman scattering peak of KS phase by several wavenumber to low frequency and the broads Raman peaks in the low frequency region. Moreover, the above two processes were reversible. The Raman analyses of the CZTS samples prepared under different process show that the PD–KS structure tends to be found at low temperatures and low sulfur vapor pressures. Our results reveal that the control of the phase structure in CZTS films is feasible by adjusting the preparation process of the films.

Keywords: Cu_2ZnSnS_4 (CZTS) films, magnetron sputtering, phase transformation

PACS: 64.60.–i, 81.15.Cd, 88.40.jn **DOI:** 10.1088/1674-1056/26/4/046402

1. Introduction

High efficiency thin film solar cells based on ternary or quaternary compound semiconductors such as Cu(In, Ga)Se_2 (CIGS) have been commercialized and developed rapidly. However, Se is toxic, In and Ga are rare metals, leading to the restriction of mass production of the CIGS solar cells. In this condition, researchers have turned their attention to alternative materials with similar properties.[1] For example, Cu_2ZnSnS_4 (CZTS) stands out with promising characteristic optical properties: a band gap energy of about 1.5 eV and large absorption coefficients in the order of 10^4 cm^{-1}. Furthermore, all the constituent elements in CZTS are low-toxic and earth-abundant.[2–5] Therefore, Kesterite (Cu_2ZnSnS_4) material has attracted significant interest as a compound semiconductor suitable for applications in thin film photovoltaics as absorbing materials. At present, the highest conversion efficiency of CZTS thin film solar cells has reached 12.6%.[6,7]

The rapid improvement of the solar cell efficiency has increased the interest of this material class. However, the best reported efficiency (12.6% for $Cu_2ZnSn(S, Se)_4$) is about half of best reported efficiency of the thin-film compound solar cells such as Cu(In, Ga)Se_2 or CdTe solar cells.[8] A review of the literatures indicates that efficiency of CZTS solar cells may be limited by the non-ideal recombinations, such as the recombination at the interface between the kesterite absorber and the CdS buffer, the recombination caused by the deep-level defects or the disordered phase in the CZTS material.[9] Thus, it is quite necessary to get a deeper understanding of the physical properties of CZTS films in order to improve the efficiency of the solar cells.

The CZTS can crystallize in kesterite (KS), stannite (ST), or partially disordered KS (PD-KS) structures, and the crystal structures of which are shown in Fig. 1. KS structure has the lowest formation energy, and the ST structure only shows small differences with the KS structure in terms of the cation arrangement in the sublattice.[10] The difference of the binding-energy between KS and ST structure is quite small (only about 3 meV/atom),[11–13] and the KS structure would coexist with the ST structure in the polycrystalline CZTS thin films prepared at high temperatures.[14] However, the neutron diffraction measurements indicated that the Cu and Zn anti-occupancy defects could exist in the CZTS films without the ST phase, which can be attributed to the PD–KS phase.[15] Since Cu^{2+} and Zn^{2+} are isoelectronic, it is found the I_{211}/I_{202} is only slightly larger for KS phase, so it is difficult to distinguish between the KS and ST/PD–KS phases by x-ray diffraction.[16,17] On the contrary, Raman spectroscopy

*Project supported by the Natural Science Foundation for Youth Fund of Hebei Province, China (Grant No. A2016201087), the Specialized Research Fund for the Doctoral Program of Higher Education of China (Grant No. 20131301120003), and the National Natural Science Foundation of China (Grant Nos. 11504078 and 61504054).

†Corresponding author. E-mail: yuwei@hbu.edu.cn
‡Corresponding author. E-mail: fugs@hbu.edu.cn
§Corresponding author. E-mail: cgao@ncu.edu.cn

© 2017 Chinese Physical Society and IOP Publishing Ltd

is sensitive to the local chemical environment of the atoms, which is a potential technology to distinguish the phase structure in CZTS films.[18] In this paper, we investigate the low-temperature phase transition from KS phase to PD–KS phase in the CZTS films and also the effect of the preparation conditions on the formation of disordered phase by using Raman scattering measurement.

2. Experimental

A series of precursors for CZTS films were deposited on Mo-coated soda-lime glass (SLG) by co-sputtering of ZnS, SnS, and Cu in a sputtering chamber. The Cu was deposited by a DC source, SnS and ZnS were deposited by RF source. Before deposition, the sputtering chamber was evacuated to the pressure below 5×10^{-4} Pa. Ar was used as working gas and the pressure was maintained at 0.5 Pa during the deposition, and the deposition time were 20 min for all the targets. During the deposition, the sputtering powers for ZnS, SnS, and Cu were 150 W, 65 W, and 15 W, respectively. After the preparation of the precursors, they were subsequently annealed at temperatures ranging from 300 °C to 500 °C in sulfur atmosphere. The annealing was carried out in a two-zone furnace in which nitrogen was used as carrier gas. The annealing time was 50 mins, and the pressure of the nitrogen in the furnace was fixed at 15 Pa–20 Pa.

Raman spectras were measured by a LabRAM HR Evolution laser Raman spectrometer (made by HORIBA JobinYvon company) using 532-nm laser as the excitation source. The laser intensity was kept low enough to avoid damaging the samples.[19] The obtained Raman curves were calibrated for all experiments. All Raman spectras were fitted using Lorentzian peaks derived from measurements with excitation wavelengths of 532 nm.[18]

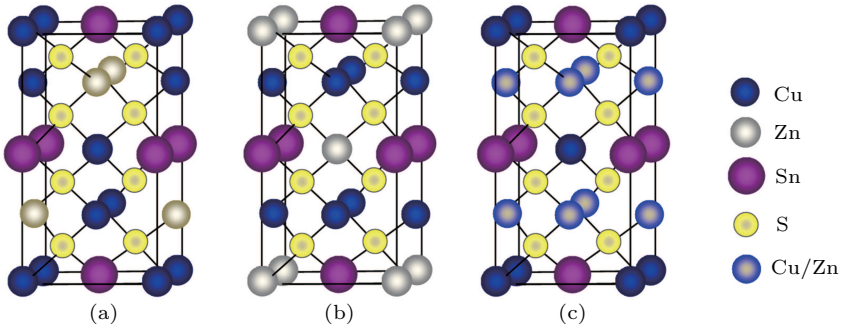


Fig. 1. (color online) Crystal structures of CZTS (a) KS-CZTS, (b) ST-CZTS, (c) PD–KS.

3. Results and discussion

3.1. Effect of laser power and heating temperature on the phase transformation of the films

Figure 2 shows the Lorentzian fitting of the Raman spectra in the range of 320 cm^{-1}–380 cm^{-1} for CZTS thin films sulfurized at 450 °C. Seven different Raman peaks are obtained by Lorentzian fitting at 322, 331, 334, 339, 348, 355, and 368 cm^{-1}, respectively.[20] The corresponding structures of the Raman peaks are shown in Table 1. Among the fitted peaks, the strongest peak is found at 339 cm^{-1}. The position of this peak matches well with the A mode of the kesterite phase of CZTS.[21–24] The peak at 331 cm^{-1} corresponds to the A_1 model of ST,[25] which is also regarded as PD–KS by Sunil K S and Valakh M Y *et al.* The PD–KS phase has the same symmetry as the ST-phase, Susanne Siebentritt *et al.* believed that the Cu/Zn disorder in CZTS films can be attributed to the existence of ST-phase . Both KS and ST structures obey octet rule whereas PD–KS does not, and Madelung energies of the three structures are KS < ST < PD − KS.[26] Therefore, it is considered that the transformation from KS to ST through PD–KS is not convincing .[12,13]

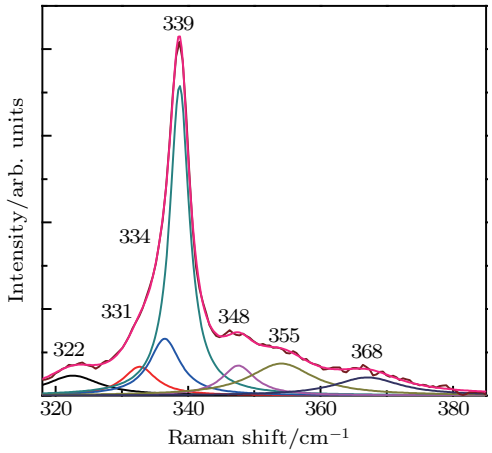


Fig. 2. (color online) Raman spectra and the Lorentzian fitting in the range of 320 cm^{-1}–380 cm^{-1}.

Table 1. Typical Raman peaks of the phases exist in the CZTS material.

Peak position/cm^{-1}	Phase	References
322	Cu_4SnS_4	[13]
331	PD–KS/ST	[12], [13], [18], [27]
334	Cu_2SnS_3	[13]
339	KS	[13], [12], [28]
348	ZnS	[23], [27]
355	Cu_2SnS_3	[23], [27], [28]
368	CZTS	[23], [27]

The Raman peak of CZTS thin films at around 331 cm^{-1} indicates the Cu–Zn disorder, i.e., the existence of Pd–KS phase. Jonathan Scragg *et al.* used the near-resonance Raman method to investigate the phase transition of CZTS, the transition temperature was estimated to be at 533±10 K. In order to study the phase transition, Raman spectra of CZTS thin films were measured at different laser powers.

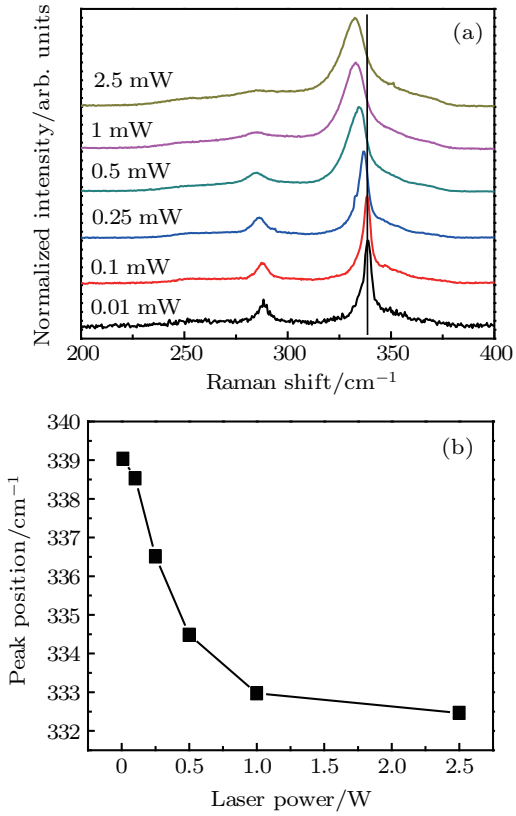


Fig. 3. (color online) (a) The Raman spectra of the sample illuminated with different laser powers, (b) the intensity variation of the peak at 339 cm^{-1} as a function of the laser powers.

The phase transition of CZTS can be analyzed by Raman spectra, and the Raman peak of CZTS thin films at around 331 cm^{-1} indicates the Cu–Zn disorder, i.e. the existence of PD–KS phase.[18] Figure 3(a) shows the Raman spectra of sample illuminated at different laser powers. It is clearly shown that the main peak of the Raman spectrum moves to the lower wavenumber as the laser power increases from 0.01 mW to 2.5 mW. Figure 3(b) shows the variation of the Raman peak intensity at 339 cm^{-1} as a function of laser powers. The intensity of the Raman peak decreases rapidly when the laser power increases from 0.01 mW to 1.0 mW, and then decrease slowly by further increasing the laser power. In order to explain this phenomenon, the Raman spectras are fitted. It is assumed that KS and PD–KS structures have similar Raman cross-sections. The ratio $R = I_{339}/I_{331}$ (i.e., the ratio between the integral area of the Raman peak at 339 cm^{-1} and 331 cm^{-1}) is used to estimate the proportion of the two phases in the sample. From Fig. 4(a), it can be seen that the PD–KS phase is observed at 331 cm^{-1} at low power (0.01 mW). By increasing the laser power, the Raman peak intensity of the PD–KS phase increases and the peak intensity of the KS phase decreases. As can be seen from Fig. 4(b), the Raman peak of the KS phase is nearly not visible when the laser power is 1 mW. This provides an important and direct evidence that the laser annealing could induce the phase transition from KS to PD–KS. The random occupancy of Cu and Zn in the lattice of CZTS is one of the reasons for the formation of the PD–KS phase, but the actual mode of the occupancy is unclear as the lattice sites occupied by Cu and Zn is almost the same.[29,30] In addition, for the materials with low thermal conductivity, the local thermal effect of the laser irradiation also makes the atoms disordered in the lattice, thus induces the phase transformation from KS to PD–KS.[31] Laser irradiation drives the system change from a lower symmetry $(I(\bar{4}))$ state to a higher symmetry $(I(\bar{4})2m)$ state.[13] Moreover, we repeated the Raman measurements at the same position of the samples using different laser power, the result of which indicates that the laser induced phase transition of CZTS is reversible.

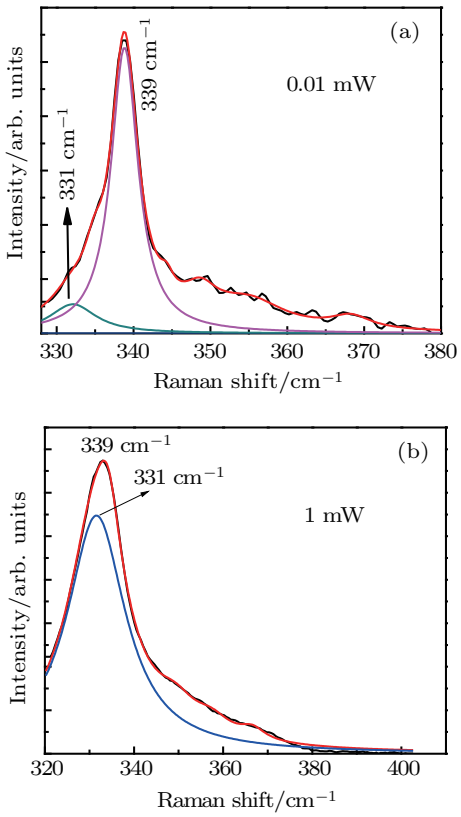


Fig. 4. (color online) The Lorentzian fitting of Raman spectra at different laser powers: (a) 0.01 mW, (b) 1 mW.

The change of the phonon frequency and full width at half maximum (FWHM) at different temperatures can provide information about the micro-structure.[20,21,32] In order to further understand the phase transformation of CZTS at low temperatures, the analysis on the temperature dependent Raman spectra is carried out. Previously, temperature dependent Raman studies of different materials have been reported, including $CuInSe_2$, GaAs, etc.

Figure 5(a) shows that the Raman spectra of CZTS samples at different temperatures. As we discussed above, the strongest peak at 339 cm^{-1} could be assigned as A mode of KS phase.[23,24] It can be seen that the A mode moves to low wavenumbers (Fig. 5(b)) with increasing the temperature, while the FWHM of the spectra increases. The grain size of the sample is far larger than the Bohr radius (2.5 nm–3.4 nm), so the shift of the peak position can not be explained by the confinement effect.[13] Prashant Sarswat *et al.* used the perturbation model to explain the increase of the phonon frequency with decreasing the temperature, and they believed that the frequency shift was caused by the combined effects of thermal expansion and the coupling to other phonons, whereas the broadening of the peaks was only caused by the anharmonic effect.[30]

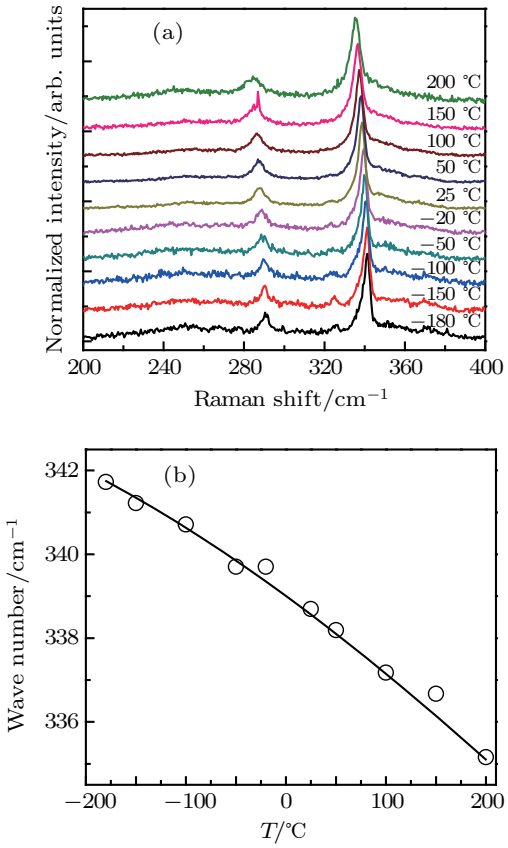


Fig. 5. (color online) (a) The Raman spectra of sample at different temperatures, (b) the variation of position of A mode with different temperatures.

Jonathan S *et al.* revealed that the transition temperature from KS to PD–KS phase was 533±10 K.[18] We compared the Lorentzian fitting of the Raman spectra measured at room temperature and 200 °C (Fig. 6), and found that the ratio R ($R = I_{339}/I_{331}$) was approximately the same. This indicates that simple heating without strong laser illumination could not result in significant phase transition. The heating only induces the shift of the Raman peak by 3 $cm^{-1} \sim 4$ cm^{-1} and broaden of the full width at half maxmum (FWHM). In addition, the repeated Raman measurements at the same position of the sample under different temperature reveal that the shift and broadeding of the Raman peaks caused by the temperature is reversible.

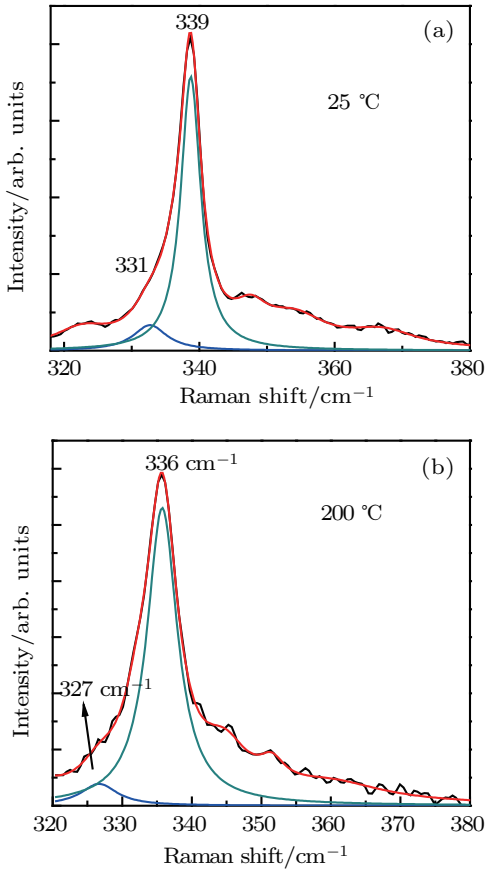


Fig. 6. (color online) The Lorentzian fitting of Raman spectra at various temperatures: (a) 25 °C, (b) 200 °C.

3.2. Effect of preparation conditions on phase transformation of the films

The presence of the PD–KS phase will decrease the efficiency of the CZTS solar cell, so it is very important to study how the preparation condition influences the formation of this phase. For this purpose, Raman spectra of the CZTS thin films prepared at different sulfurization temperture and sulfurization pressure were investigated.

Figure 7(a) gives the five values of R ($R = I_{339}/I_{331}$) at different sulfurization temperatures of 300 °C, 350 °C, 400 °C, 450 °C, 500 °C, respectively. It can be seen that the value of R increases with increasing the temperature. The reason is that the KS structure has lower strain energy and Madelung energy as compared with ST structure and PD–KS structure, so that the KS structure is the most stable phase among the three structures. This indicates that surfurization at high temperatures is beneficial to the formation of KS structure in CZTS. Moreover, the FWHM of Raman peaks at 331 cm^{-1} and 339 cm^{-1} (not shown) decrease as the sulfurization temperature increases, indicating an improvement of the crystallinity in the material.

The change of R values as the sulfurization pressure is shown in the Fig. 7(b). It can be seen that the R value decreases with the increase of the sulfurization pressure, which indicates that the proportion of KS phase in CZTS decreases

with increasing the sulfurization pressure. The experimental result indicates that a higher sulfur partial pressure could contribute to the formation of KS structure in CZTS. Meanwhile, the FWHM of Raman peaks at 331 cm^{-1} and 339 cm^{-1} (not shown) increase with the increase of the sulfurization pressure, indicating that the crystallinity of the KS and PS–KS phase decreases with the increase of the sulfurization pressure. The reason could be that the sulfur partial pressure in the vacuum pipe decreases with increasing the sulfurization pressure, so that the following reaction would shift to the right side, leading to the decrease of the crystal quality of the CZTS films.

$$\mathrm{Cu_2(S,Se)_{(s)} + Zn(S,Se)_{(s)} + Sn(S,Se)_{(g)} + S_{2(g)}} \leftrightarrow \mathrm{Cu_2ZnSn(S,Se)_4}.$$

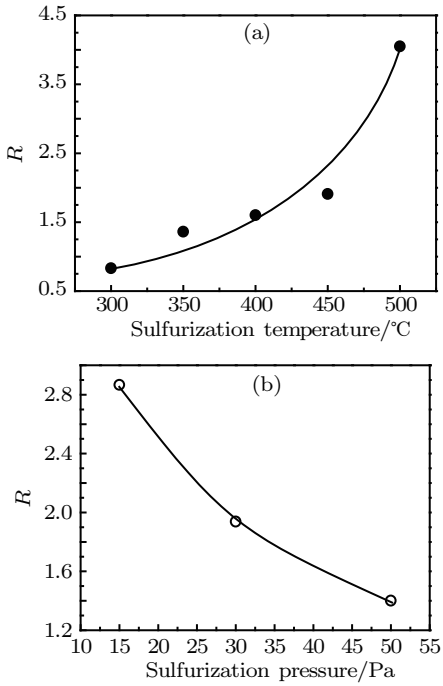


Fig. 7. The variation of ratio R with the change of (a) sulfurization temperature and (b) sulfurization pressure.

4. Conclusions

In this paper, the low-temperature phase transformation from KS phase to PD–KS phase in CZTS thin films was investigated by laser annealing and low temperature thermal annealing. A series of CZTS precursors were deposited on Mo-coated soda-lime glass (SLG) by co-sputtering of ZnS, SnS and Cu. Subsequently, the samples were annealed at sulfurization temperatures ranging from 300 °C to 500 °C and sulfurization pressures ranging from 15 Pa to 50 Pa. We analyzed the Raman spectra of sample illuminated at different laser powers. The result show that the Raman scattering peak of the KS phase is red shifted and the Raman peak of the PD–KS phase emerges with increasing the laser power. However, simple low temperature heating without strong laser illumination could not induce significant phase transition, but only shifts the Raman scattering peak of KS phase shift to the lower wavenumbers by several wavenumber and broaden the FWHM. We also find the change of the micro-structures induced by laser or simple heating are both reversible. Moreover, the Raman spectra of samples prepared at sulfurization temperatures of 300 °C–500 °C and pressure of 15 Pa were studied. The results demonstrates that the high temperature and high sulfur partial pressure could lead to the formation of KS. Therefore, it could be feasible to control the phase transition in CZTS films.

References

[1] Fernandes P A, Salomé P M P and Cunha A F D 2009 *Thin Solid Films* **517** 2519
[2] Chan C P, Lam H and Surya C 2010 *Sol. Energy Mater. Sol. Cells* **94** 207
[3] Friedlmeier T M, Wieser N, Walter T, Dittrich H and Schock H W 1997 *Proceedings of the* 14*th European Photovotlaic Specialists Conference Barcelona*, 1997, Spain, p. 1242
[4] Raulot J M, Domain C and Guillemoles J F 2005 *Phys. Rev. B* **71** 035203
[5] Friedlmeier T A M 2001 *Fortschritt-Berichte VDI Reihe 9 Nr.* **340** 122
[6] Katagiri H, Jimbo K, Maw W S, Oishi K, Yamazaki M, Araki H and Takeuchi A 2009 *Thin Solid Films* **517** 2455
[7] Wang W, Winkler M T, Gunawan O, Gokmen T, Todorov T K, Zhu Y and Mitzi D B 2014 *Adv. Energy Mater.* **4** 403
[8] Green M A, Emery K, Hishikawa Y, Warta W and Dunlop E D 2012 *Photovolt. Res. Appl.* **20** 606
[9] Siebentritt S 2013 *Thin Solid Films* **535** 1
[10] Samji S K, Tiwari B, Surendra M K and Rao M R 2014 *Appl. Phys. Lett.* **104** 152106
[11] Walsh A, Chen S, Wei S H and Gong X G 2012 *Adv. Energy Mater.* **2** 400
[12] Siebentritt S and Schorr S 2012 *Prog. Photovolt: Res. Appl.* **20** 512
[13] Valakh M Y, Kolomys O F, Ponomaryov S S, Yukhymchuk V O, BabichukI S, Izquierdo-Roca V, Saucedo E, Perez-Rodriguez A, Morante J R, Schorr S and Bodnar I V 2013 *Phys. Status Solidi (RRL)* **7** 258
[14] Khare A, Himmetoglu B, Johnson M, Norris D J, Matteo C and Eray S A 2012 *Appl. Phys.* **111** 083707
[15] Schorr S 2011 *Sol. Energy Mater. Solar Cells* **95** 1482
[16] Siebentritt S and Schorr S 2012 *Prog. Photovolt: Res. Appl.* **20** 512
[17] Schorr S and Gonzalez-Aviles G 2009 *Phys. Status Solidi* **206** 1054
[18] Jonathan J S S, Leo C, Alain L, Tove E and Charlotte P B 2014 *Appl. Phys. Lett.* **104** 041911
[19] Valakh M Y, Dzhagan V M, Babichuk I S, Fontane X, PerezRodriquez A and Schorr S 2013 *JETP Lett.* **98** 255
[20] Wang W, Shen H L, Jin J L, Li J Z and Ma Y 2015 *Chin. Phys. B* **24** 056805
[21] Himmrich M and Haeuseler H 1991 *Spectrochim. Acta* **47** 933
[22] Aroyo M I, Perez-Mato J M, Capillas C, Kroumova E, Ivantchev S, Madariaga G, Kirov A and Wondratschek H 2006 *Z. Kristallogr* **221** 15
[23] Fernandese P A, Salome P M. P and Cunha A F D 2009 *Thin Solid Films* **517** 2519
[24] Altosaar M, Raudoja J, Timmo K, Danilson M, Grossberg M, Krustok J and Mellikov E 2008 *Phys. Status Solidi A* **205** 167
[25] Ankur K, Burak H, Melissa J, David J N, Matteo C and Eray S A 2012 *J. Appl. Phys.* **111** 083707
[26] Su D S, Neumann W and Giersig M 2000 *Thin Solid Films* **361–362** 218
[27] Dimitrievska M, Fairbrother A, Fontane X, Jawhari T, Izquierdo-Roca V, Saucedo E and Pérez-Rodríguez A 2014 *Appl. Phys. Lett.* **104** 02190
[28] Grossberg M, Krustok J, Raudoja J and Raadik T 2012 *Appl. Phys. Lett.* **101** 102102
[29] Schorr S 2011 *Sol. Energy Mater. Sol. Cells* **95** 1482
[30] Schorr S, Hoebler H J and Tovar M 2007 *Eur. J. Mineral* **19** 65
[31] Yang H, Jauregui L A, Zhang G, Chen Y P and Wu Y 2012 *Nano Lett.* **12** 540
[32] Sarswat P K, Free M L and Ashutosh T 2011 *Phys. Status Solidi* **248** 2170